Differential Cytotoxicity of Human Wild Type and Mutant α-Synuclein in Human Neuroblastoma SH-SY5Y Cells in the Presence of Dopamine[†]

Charbel E.-H. Moussa,[‡] Christophe Wersinger,[‡] York Tomita,[§] and Anita Sidhu*[,‡]

Departments of Pediatrics and Oncology, Georgetown University, Washington, D.C. 20007

Received November 25, 2003; Revised Manuscript Received January 11, 2004

ABSTRACT: Parkinson's disease (PD) involves loss of dopaminergic neurons in the substantia nigra and is characterized by intracellular inclusions, Lewy bodies, consisting primarily of aggregated α-synuclein. Two substitution mutations (A53T and A30P) in α-synuclein gene have been identified in familial early-onset PD. To understand the biological changes that incur upon α-synuclein-induced cytotoxicity in the presence of dopamine, the current studies were undertaken. Human SH-SY5Y neuroblastoma cells coexpressing the human dopamine transporter [hDAT], and either wild type (wt) or mutant α-synucleins, were treated with 50 μM dopamine (DA). In cells expressing wt or A30P α-synuclein, DA accelerated production of reactive oxygen species and cell death as compared to cells expressing A53T or hDAT alone. The increased sensitivity of such cells to DA was investigated by measuring changes in cellular ionic gradient, by atomic absorption spectrometry, and cell metabolism, by high-resolution nuclear magnetic resonance spectroscopy. Both wt and A30P α-synuclein caused rapid decrease in levels of intracellular potassium, followed by mitochondrial damage and cytochrome *c* leakage, with decreased cellular metabolism as compared to cells expressing A53T or hDAT alone. Collapse of ionic gradient was significantly faster in A30P ($t_{1/2}$ = 3.5 h) than in wt ($t_{1/2}$ = 6.5 h) cells, and these changes in ionic gradient preceded cytochrome *c* leakage and depletion of metabolic energy. Neither wt nor mutant α-synuclein resulted in significant changes in ionic gradient or cellular metabolism in the absence of intracellular DA. These findings suggest a specific sequence of events triggered by dopamine and differentially exacerbated by α-synuclein and the A30P mutant.

Parkinson's disease (PD)[1] is a neurodegenerative movement disorder characterized by a loss of dopaminergic neurons in the substantia nigra and the accumulation of fibrous protein deposits, consisting primarily of α-synuclein, in neuronal cytoplasm (Lewy bodies) and nerve fibers (Lewy neurites) in the brain (*1*−*5*). Human wt α-synuclein forms inclusions into LBs in transgenic mice and *Drosophilia* (*6*, *7*). PD patients show an increased level of oxidative damage to DNA, lipids, and proteins (*8*−*12*), and dopamine (DA) metabolism or oxidative phosphorylation produce reactive oxygen species (ROS), which is likely responsible for this oxidative damage (*13*, *14*). Additionally, several lines of evidence suggest a central role for the process of α-synuclein fibrillization in oxidative stress (*15*−*19*). Oxidatively modified α-synuclein is more prone to aggregation than native protein (*20*), and α-synuclein was reported to catalyze the formation of hydrogen peroxide in vitro (*21*). Therefore, the ability of DA to produce ROS, and the effects of DA and ROS on α-synuclein function and aggregation suggest a close relationship between this protein and DA in the selective death of neurons that produce DA (*22*−*25*).

Two different α-synuclein substitution mutations (A30P and A53T) are associated with rare, autosomal dominant, early-onset PD (*26*, *27*). Both mutations accelerate α-synuclein aggregation (*28*−*30*), and promote the conversion of protofibrils into fibrils, suggesting that protofibrils, rather than fibrils, are linked to cytotoxicity (*19*, *30*−*32*). Moreover, oxidized DA and its metabolites were shown to stabilize the formation of protofibrils of α-synuclein (*33*). However, although the A53T mutant is the fastest to fibrillize (*28*, *31*, *34*), the A30P variant is the most toxic form of α-synuclein, followed by wt and A53T (*34*−*36*), perhaps due to protracted exposure to toxic protofibrils in the presence of the A30P mutant. However, low expression levels of α-synuclein protect against cytotoxicity, while high expression levels induce oxidative stress and cell death (*37*−*39*). The relationship between DA and α-synuclein seems also to be dictated by the interaction between α-synuclein and hDAT. Regulation of hDAT activity by α-synuclein has been reported to be via direct physical and functional interaction (*40*, *41*). In addition, α-synuclein and its mutants variably regulate hDAT activity (*42*). The A30P mutant negatively modulates func-

[†] This study was supported by grants from the National Institutes of Health [NS-34914 and NS-45326].

* Corresponding author. Tel.: (202) 687-0282. Fax: (202) 687-0279. E-mail: sidhua@georgetown.edu.

[‡] Department of Pediatrics.

[§] Department of Oncology.

[1] Abbreviations: PD, Parkinson's disease; LBs, Lewy bodies; hDAT, human dopamine transporter; wt, wild type; DA, dopamine; NMR, nuclear magnetic resonance; ROS, reactive oxygen species; TCA, tricarboxylic acid cycle; Glu, glutamate; Cit, citrate; Succ, succinate; Lac, lactate; Ala, alanine; ATP, adenosine trisphosphate; MTT, 3-[4,5-dimethylthiazol-2-yl]-2,5-diphenyl-tetrazolium bromide; DCF, 2′,7′-dichlorodihydrofluorescein diacetate; T2, 2 μg of hDAT DNA; T2S2, 2 μg of hDAT and 2 μg of wt α-synuclein DNA; T2S10, 2 μg of hDAT DNA and 10 μg of wt α-synuclein DNA; T2T10, 2 μg of hDAT and 10 μg of A53T mutant DNA; T2P10, 2 μg of hDAT and 10 μg of A30P mutant DNA.

10.1021/bi036114f CCC: $27.50
Published on Web 04/10/2004

tional activity of hDAT to a greater extent than wt α-synuclein, with reduced uptake of extracellular DA, while the A53T mutant has no significant effect on dopamine uptake (*42*).

The current studies were undertaken to better understand the cytotoxic effects of high expression levels of α-synuclein and its mutants in the presence of intracellular DA. The data presented here show that α-synuclein and its mutants differentially exacerbate production of ROS leading to significant changes in cellular ionic gradient, profoundly altering mitochondrial function and depressing cellular metabolism, in the presence of DA and in a manner dependent on the expression levels of these proteins. Moreover, the data show that both the wt and its A30P mutant are much more cytotoxic than the A53T variant. These studies provide a novel insight into a possible mechanism of pathophysiological staging of the progression of cytotoxicity induced by high levels of human wt and mutant α-synuclein in the presence of intracellular DA.

EXPERIMENTAL PROCEDURES

DNA, Cell Culture, and Transfection. Human α-synuclein cDNA (gift from T. Dawson) and hDAT cDNA (gift from H. B. Niznik and F. Liu) were subcloned into the mammalian expression vector pcDNA3.1 (Invitrogen) using the *EcoRI* restriction site. Plasmid DNAs were propagated in *Escherichia coli* DH5α and purified from overnight bacterial cultures using the Endo-Free Plasmid Mega kit from Qiagen Inc. (Valencia, CA). Human neuroblastoma SH-SY5Y cells (seeding density 2×10^5 cells) were grown in T75 cm^2 flasks in DMEM (Life Technologies) + 10% (vol/vol) heat-inactivated selected FBS (Sigma), antibiotics, and 2 mM l-glutamine at 37 °C and 5% CO_2 until 80% confluence, then transiently transfected [2−10 μg of DNA/2×10^5 cells] using Lipofectamine 2000 (Invitrogen) and Opti-MEM (Invitrogen) without serum, according to Invitrogen's protocol. For all experiments, the final quantity of DNA used during transfection was identical and kept constant by adjusting with a pcDNA3.1 control vector that lacked a cDNA insert. Four to six hours after transfection, DMEM + 10% FBS was added, and cells were further grown for 2 days to allow expression of the transgenes. [^{3}H]DA uptake studies and Western blot analyses were conducted as previously described by Wersinger et al. (*41*, *42*). All pellets in these studies were collected for protein estimation by the Lowry technique. Cells were detached with trypsin−versene solution (0.1% trypsin, 0.53 mM EDTA-4Na in Hank's balanced solution without Ca and Mg; Sigma) and centrifuged at 1000 rpm for 5 min to precipitate the cells and then resuspended in different solutions as indicated next. Throughout these studies, DA was added in the absence of serum to the treatment medium.

Primary Rat Mesencephalic Neuronal Cultures. Mesencephalons from 18 day old rat embryos were isolated, and the cells were dissociated by mechanical disruption by repetitive pipeting through a Pasteur glass pipet, counted (700 cells seeded/mm^2), and grown at 37 °C and 5% CO_2 in Neurobasal medium (Life Technologies) supplemented with 2% (v/v) B-27 supplement (Life Technologies) and 50 μM of β-mercaptoethanol (Sigma) on glass cover-slips precoated with poly-L-ornithine (15% w/v in 0.1 M borate buffer, pH 8.4; Sigma) and laminin (3 μg/mL in PBS; Sigma) for 10 days. Culture media used to grow the neuronal cultures were changed every second day.

Cell Viability (MTT) Assay and ROS Production (DCF Assay). Human neuroblastoma SH-SY5Y cells were grown and transfected as described previously in 6 well dishes and treated with 50 μM DA for 16 h. Cells were washed twice in warm D-PBS and incubated either in 1 mL of DMEM (no serum) containing 0.5 mg of (3-[4,5-dimethylthiazol-2-yl]-2,5-diphenyl-tetrazolium bromide (MTT) for 2−3 h at 37 °C and 5% CO_2 or in 1 mL of DMEM (no serum) containing 100 μM 2′,7′-dichlorodihydrofluorescein diacetate (DCF; Molecular Probes, Eugene, OR) for 45 min at RT. DMEM containing MTT was aspirated, cells were carefully washed twice with warm D-PBS at RT, and formazan salts were dissolved in 1 mL of pure ethanol. Cells were homogenized by repetitive pipeting and centrifuged for 5 min at 4500 rpm, the supernatant was collected by careful decanting to avoid redissolving the protein pellet in ethanol, and absorbance was read against an ethanol blank at 564 nm. ROS production was measured at 525 nm (excitation at 475 nm) in a microplate reader (CytoFluor 2350, Millipore).

Cell Culture Treatment and Preparation of NMR Samples. Cells were grown (transfected as indicated previously) in triplicate to increase the concentration of each sample to the degree of sensitivity allowed by NMR in T175 cm^2 flasks (NUNC) to 95% confluence in DMEM + 10% FBS, washed twice in PBS, and reincubated in DMEM (Sigma D-5030) to starve them in the absence of serum, l-glutamine, glucose, and sodium pyruvate (treatment medium for NMR samples) for 2−3 h at 37 °C and 5% CO_2. Following starvation, which is essential to rid the cells of endogenous glucose, 2 mM [3-^{13}C]sodium pyruvate (Cambridge Isotopes) was added to the treatment medium, 2−3 h before treatment with 50 μM DA, to allow cells to incorporate the labeled carbon. After 16 h of treatment with 50 μM DA, cells were harvested with trypsin−versene solution (Sigma) and centrifuged at 1000 rpm for 5 min to precipitate the cells, and the supernatant was discarded. The pellets were resuspended, homogenized by mild sonication, and extracted in ice-cold 5% perchloric acid (PCA). The homogenates were centrifuged for 15 min at 4 °C and 4500 rpm, and the extracts were neutralized to pH 7.2 with KOH. After neutralization, the supernatants were centrifuged again for 15 min at 4 °C and 4500 rpm to remove salts and then lyophilized. Lyophilized supernatants were resuspended in 0.65 mL of D_2O containing 2 mM sodium [^{13}C]formate as an internal intensity and chemical shift reference (δ 171.8) and stored at −20 °C until required for NMR analysis.

NMR Analysis. NMR analysis was performed using [^{1}H-decoupled]^{13}C observed spectra (22 000 transients, duty cycle 4 s, 83 300 data points) at 9.4 T, on a Bruker AVANCE DMX-400 spectrometer using a 5 mm QNP W1 probe with XYZ-gradient. Fully relaxed ^{1}H and [^{13}C-decoupled]^{1}H spectra (16 transients) were obtained on a Bruker DMX-600 spectrometer using an MPF7 composite pulse decoupling sequence with a TX1 600 S3 cryoprobe (H-C/N-D-052). Assignments were aided by reference to standard spectra. Following zero-filling to 128 000 (data points), [^{1}H-decoupled] ^{13}C spectra were transformed using 3 Hz exponential line-broadening, and peak areas determined by integration

using standard Bruker software (XWINNMR, Version 2.6). Peak areas were adjusted for nuclear Overhauser effect, saturation, and natural abundance effects and quantified by reference to the area of the internal standard resonance of [^{13}C]formate. Metabolite pool sizes were determined by integration of resonances in fully relaxed 600 MHz [^{13}C-decoupled] ^{1}H spectra using [^{13}C]formate as the internal intensity reference. Numbering of carbon atoms is as described by Sonnewald et al. (*43*).

Preparation of Samples for HPLC Analysis. High performance liquid chromatography was performed to quantify leakage of cytochrome *c* from mitochondria into cytosol. To extract the cytosolic fraction of cellular contents, cells were lysed by hyposmolarity for 5 min in 0.5 mL of distilled deionized (18.2 mΩ/cm resistivity, Millipore) water containing protease inhibitor cocktail at 1 mL/100 mL of cell lysate (Sigma) and centrifuged for 30 min at 18 000 rpm and 4 °C, and the supernatant containing cytoplasmic fraction was collected. To extract the mitochondrial fraction, the pellets were resuspended in 0.5 mL of distilled deionized water containing protease inhibitor cocktail and homogenized by sonication on ice 5 times for 10 s with 5 s pauses, and cell lysates were centrifuged for 30 min at 18 000 rpm and 4 °C. High performance liquid chromatography was performed with Amersham Pharmacia Biotech, Purifier 10 (AKTA design), using PRP-3 (4.1 × 150 mm) reversed phase column (Hamilton Company, Reno, NV), with condition (A) 0.1% trifluoroacetic acid (TFA) in water pH 2.0 and condition (B) 0.1% TFA in acetonitrile with a linear gradient 0−50% in 30 min at 0.5 mL/min, ambient, UV at 215 nm. The chromatograms were integrated using UNICORN V3.21 software.

Atomic Absorption Spectrometry. To measure intracellular potassium concentration in cytosolic fractions, atomic absorption spectrometry was performed using a potassium hollow cathode lamp (Buck Scientific 200A) with single beam operating/max current 1/8 with acetylene as fuel and air as support. The flame stoichoimetry was adjusted to oxidizing position. Wavelength was selected at 766.9 nm and the slit width of the spectrometer at 0.1 nm.

RESULTS

Differential Cytotoxicity of wt α-Synuclein and its Mutants when Expressed at High Levels. We have previously shown that at low expression levels, reminiscent of that seen in substantia nigra (Wersinger et al., unpublished observations), α-synuclein and its A30P mutant [2 μg of DNA] diminished the uptake of DA by hDAT [2 μg of DNA] in L*tk*$^{-}$ fibroblasts, which was accompanied by reduced cytotoxicity and oxidative stress, as compared to cells expressing hDAT alone [2 μg of DNA, refs *40*−*42*]. Interestingly, the A53T mutant [2 μg of DNA] did not significantly alter these parameters, as compared to cells expressing hDAT alone (*42*).

To examine the effect of high expression levels of wt α-synuclein in the induction of cytotoxicity, human neuroblastoma SH-SY5Y cells were transiently transfected with a constant amount of hDAT DNA [2 μg, T2 cells] and with either 2 μg [T2S2 cells] or 10 μg [T2S10 cells] of wt α-synuclein DNA. In parallel studies, cells were also cotransfected with 2 μg of hDAT DNA and 10 μg of the A30P [T2P10 cells] or 10 μg of the A53T [T2T10 cells] mutant DNA. [^{3}H]DA uptake studies were conducted (Figure 1A) to measure the initial [^{3}H]DA uptake velocity in SH-SY5Y neuroblastoma cells, and in the presence of high expression levels of A30P and wt α-synuclein, there was significant attenuation of [^{3}H]DA uptake, by 65 and 55%, respectively. By contrast, in T2T10 cells expressing the A53T α-synuclein, the mutant caused the least amount of inhibition of [^{3}H]DA uptake [30%], which was not significantly different from either that of T2S2 or T2 cells. In control studies with mock transfected cells (pcDNA3.1 vector alone), there was no [^{3}H]DA uptake into these cells, and treatment with 10 μM hDAT inhibitor indatraline (INDT) completely blocked [^{3}H]DA uptake, indicating the hDAT specificity of the uptake.

To measure the effects of reduced uptake of [^{3}H]DA by hDAT in the presence of wt and mutant α-synucleins on oxidative stress via production of ROS, we measured ROS production in the various α-synuclein expressing cells, after exposure of these cells to 50 μM dopamine for 16 h. As compared to mock transfected cells, ROS production was significantly increased (100%) in T2 cells (Figure 1B). However, at low expression levels of wt α-synuclein (T2S2 cells), there was significant attenuation [50%] in ROS production, as compared to the T2 cells, similar to our previous findings in L*tk*$^{-}$ fibroblasts (*41*). Surprisingly, at higher levels of α-synuclein expression in T2S10 cells, there was a significant [$p < 0.05$] increase of 150% in ROS production, as compared to mock transfected cells, despite the diminished uptake of DA in these cells. Moreover, this increase in ROS in T2S10 cells was significantly higher than that seen in either T2S2 [by 100%] or in T2 cells.

The mutants also increased ROS production, and in both T2T10 cells and in T2P10 cells, ROS levels were 125 and 200%, respectively, higher than that seen in mock transfected cells. Moreover, these levels of ROS were also significantly [$p < 0.05$] higher than that seen in T2 cells, while ROS production in T2P10 cells was higher than that of T2S10 cells. Interestingly, the increased ROS production in T2T10 cells was higher than that of T2 cells, despite both these cells having similar uptake of DA.

We next measured cell viability, indexed by MTT assays, as described in Experimental Procedures. In all instances, cell death paralleled the production of ROS (Figure 1C). Thus, DA decreased cell viability in T2 cells by more than 50%. In T2S2 cells there was a significant decrease of cell death relative to T2 cells, after 16 h treatment with DA, reminiscent of our earlier findings in L*tk*$^{-}$ fibroblasts (*41*). At higher expression levels, however, cell viability was sharply reduced, and the most dramatic effects on cell viability were observed in T2P10 cells (90%), followed by T2S10 (75%) and T2T10 (60%).

Additionally, Western blot analysis (Figure 1D) showed that the expression levels of α-synuclein and the A30P and A53T mutants did not change over the period of treatment with DA (upper panel, lanes 1−4 = 2 h and lanes 5−8 = 16 h; lower panel, lanes 1−4 = 4 h and lanes 5−8 = 8 h), suggesting no effects on expression levels of α-synuclein proteins as a consequence of treatment with DA.

To eliminate the possibility that increased expression of the various α-synuclein variants may have caused differential expression of hDAT, thereby resulting in diminished uptake of [^{3}H]DA in these studies, we examined the expression

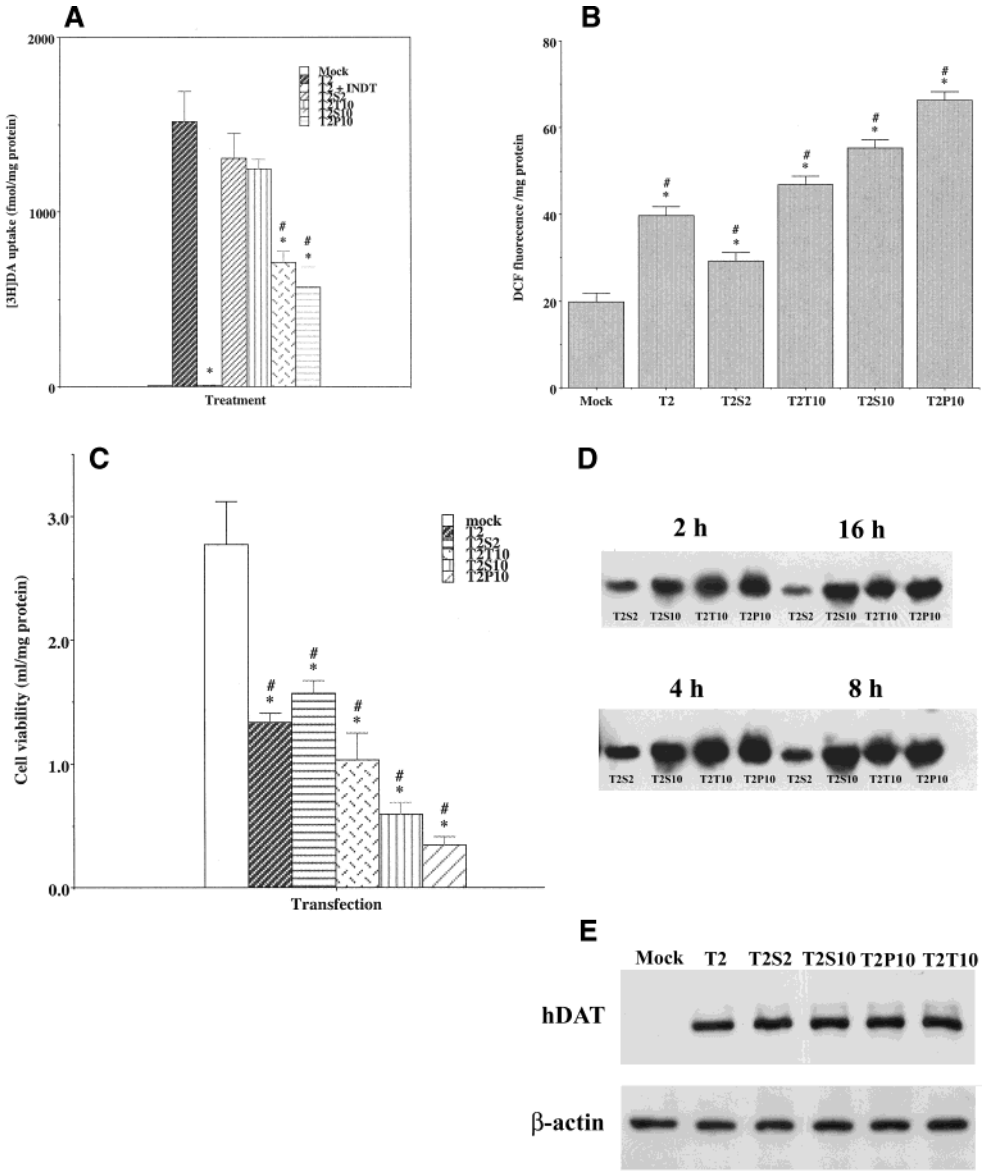

FIGURE 1: Histograms show [^{3}H]DA uptake (A), ROS production (B), and cell viability (C) in SH-SY5Y cells treated with 50 μM DA for 16 h (B and C). *Significantly different to T2 and # significantly different to T2S2 (A). *Significantly different to control (B and C) and # significantly different to all other treatments (B) and significantly different to preceding treatment on the graph (C). INDT: indatraline. ANOVA, 95% confidence, Fisher PLSD. Mean ± SD based on n = 12, 8, and 5 for panels A−C, respectively. Expression levels of α-synuclein and mutants (D) on a NuPAGE peptide gel (upper panel: lanes 1−4 = 2 h and lanes 5−8 = 16 h and lower panel: lanes 1−4 = 4 h and lanes 5−8 = 8 h treatment with 50 μM DA. Expression levels of hDAT (E) in a 10% polyacrylamide gel (30 μg protein/lane), seen as a band of MW ~85 kDa. The lower gel in panel E shows β-actin immunoreactivity in each lane, used to confirm equal protein loading. Data shown in panels D and E are representative of n = 3 independent experiments.

levels of hDAT protein in the various transfectants by Western blots. As seen in Figure 1E, the hDAT protein levels were unchanged in cells transfected with either low [2 μg of cDNA] or high [10 μg of cDNA] amounts of α-synuclein and its mutants. These data suggest that the cytotoxicity observed in cells expressing high levels of either wt α-synuclein or its mutants is not due to changes in hDAT or α-synuclein expression levels and is also not solely related to increased uptake of DA into the cells since even under reduced levels of DA uptake both ROS production and cell death were increased under these conditions. Rather, the combined data suggest that wt and mutant forms of α-synuclein in the presence of DA may differentially trigger cytotoxicity.

Wild Type and Mutant α-Synuclein Differentially Induce Loss of Ionic Gradient in SH-SY5Y Cells. Fluctuations in intracellular potassium concentration indicate changes in cellular ionic gradient and possible collapse in cell homeostasis and Na^+/K^+-ATPase pump activity. We measured the cellular ionic gradient to better understand the effects of ROS production in cells expressing high levels of the α-synuclein variants on cell biochemical and metabolic properties. Intracellular potassium concentration was measured in different cells treated with 50 μM DA for 16 h, by atomic absorption spectrometry, as described in Experimental Procedures. As compared to mock-transfected cells, intracellular potassium levels were significantly decreased (Figure 2A) in T2 cells (35%), while T2S2 cells somewhat attenuated loss of intracellular potassium relative to T2 cells since in these cells only 25% loss was observed. Loss of intracellular potassium reached the highest levels in T2P10 (55%) followed by T2S10 (50%) and T2T10 (40%) cells. Inhibition

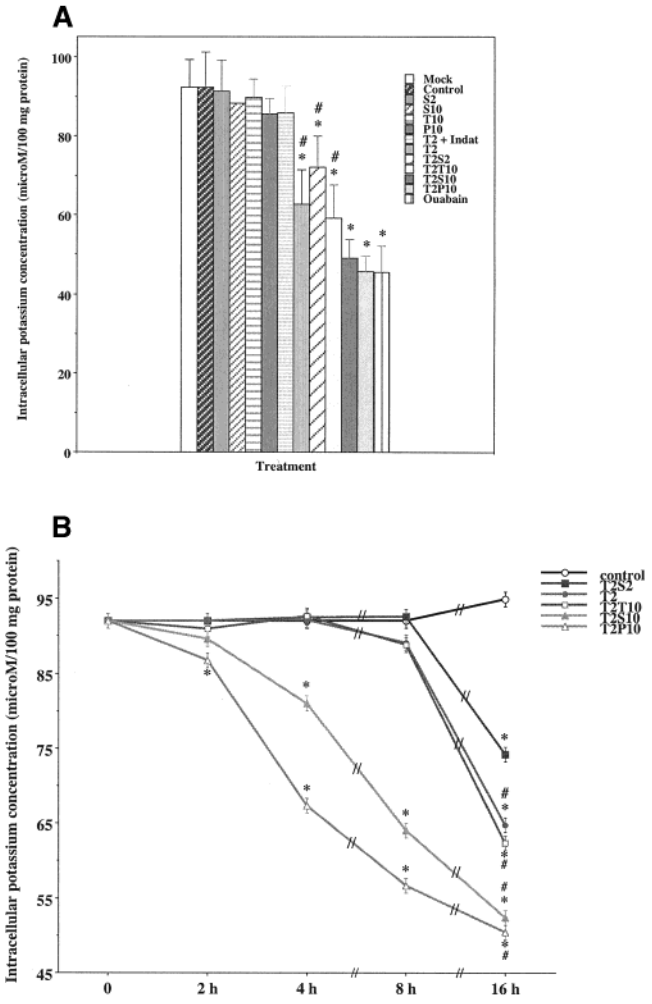

FIGURE 2: Histogram shows intracellular potassium concentration (A) in SH-SY5Y cells treated with 50 μM DA for 16 h. Graph shows temporal changes in intracellular potassium concentration in human neuroblastoma SH-SY5Y cells treated with 50 μM DA over 16 h period (B). *Significantly different to control (A and B) and # significantly different to ouabain (A) and significantly different to T2S2 (B). INDT: indatraline. ANOVA, 95% confidence, Fisher PLSD. Mean ± SD based on $n = 5$.

of the Na^+/K^+-ATPase pump with 10 μM ouabain, a classical inhibitor of Na^+/K^+-ATPase pump, in mock-treated cells resulted in a maximal 50% decrease of intracellular potassium, comparable to the effects seen in T2S10 and T2P10 cells, suggesting that the decrease in intracellular potassium seen, especially at higher expression of wt and A30P α-synuclein, results from an inhibitory effect on ionic pump activity, which is energy (ATP)-dependent. In control studies, where cells were transfected with the three variants of α-synuclein but in the absence of hDAT, or in T2 cells coincubated with the hDAT inhibitor, indrataline (INDT = 10 μM), treatment of such cells with dopamine [50 μM, 16 h] did not induce a decrease in intracellular potassium as compared to control (Figure 2A), indicating that the collapse in ionic gradient was not intrinsic to the properties of the α-synucleins per se but was dependent on the presence of intracellular DA.

The differential effects of α-synuclein on intracellular potassium after 16 h of treatment with DA prompted further investigation of temporal changes of ionic gradient. Time course studies (Figure 2B) show a significant decrease in intracellular potassium in T2P10 cells as early as 2 h and in T2S10 cells after 4 h as compared to mock-transfected and all other cells. Even after 4 and 8 h of treatment, the decreases in T2P10 occurred faster than that seen in T2S10 cells, indicating that the A30P mutant is the most potent variant of α-synuclein in altering cellular ionic gradient. Collapse of ionic gradient was significantly faster in A30P ($t_{1/2} = 3.5$ h) than in wt ($t_{1/2} = 6.5$ h) or A53T cells. No significant changes were observed in intracellular potassium concentrations after 8 h treatment in T2, T2S2, and T2T10 as compared to mock cells; however, after 16 h of treatment with DA, significant decreases of intracellular potassium were observed in these cells as compared to mock. Taken together, these data suggest a differential staging of loss of ionic gradient between wt α-synuclein and the A30P mutant, indicating a critical role for the α-synucleins in triggering changes in cellular ionic gradient and homeostasis, although with varying degrees.

Cytochrome c Leakage into Cytosol Is Secondary to Changes in Ionic Gradient. We next examined changes in mitochondrial function by measuring leakage of cytochrome *c* into the cytosol. Mitochondrial and cytoplasmic fractions of cytochrome *c* of transfected cells were isolated, after treatment of these cells with 50 μM DA for 16 h, and levels of cytochrome *c* in each fraction were quantified by RP-HPLC. A significantly increased level (Figure 3A) of cytosolic cytochrome *c* was observed in T2 cells (90%), while T2S2 cells attenuated this increase in cytochrome *c* leakage (50%). Cytosolic cytochrome *c* leakage was highest in T2P10 cells (170%), followed by T2S10 (160%) and T2T10 (95%) as compared to mock treatment. In all instances, these increases in the cytosolic fraction of cytochrome *c* were paralleled by decreases in the cytochrome *c* content of the mitochondrial fractions, suggesting loss of cytochrome *c* from mitochondria.

We next investigated temporal changes in cytochrome *c* levels in the cytosol to better understand the staging of the progression of cell death induced by the α-synuclein variants in the presence of DA. Levels of cytochrome *c* leakage into cytosol were significantly increased (Figure 3B) in T2S10 and T2P10 cells after 8 h of treatment with DA as compared to control and all other treatments, while no significant changes in cytochrome *c* levels in the cytosol were observed in T2, T2S2, and T2T10 cells until these cells were treated for 16 h with DA. Cytochrome *c* leakage into cytosol was significantly faster in A30P ($t_{1/2} = 3.5$ h) than in wt ($t_{1/2} = 6.5$ h) or A53T cells, again demonstrating the differential rate of cytotoxicity induced by the various α-synuclein variants.

Changes in Ionic Gradient Also Precede Mitochondrial Damage in Rat Primary Mesencephalic Neuronal Cultures. To test the physiological relevance of the changes we observe in SH-SY5Y cells, we also measured ionic gradient and cytochrome *c* content in endogenously expressing systems, by conducting similar studies in rat primary mesencephalic neurons, which express the dopamine transporter and α-synuclein. Treatment of these mesencephalic neurons with 10 μM DA resulted in a significant decrease in intracellular potassium as early as 2 h (Figure 4A) and continued to decrease as compared to either control neurons [up to 16 h] or to neurons treated with DA in the presence of 5 μM INDT

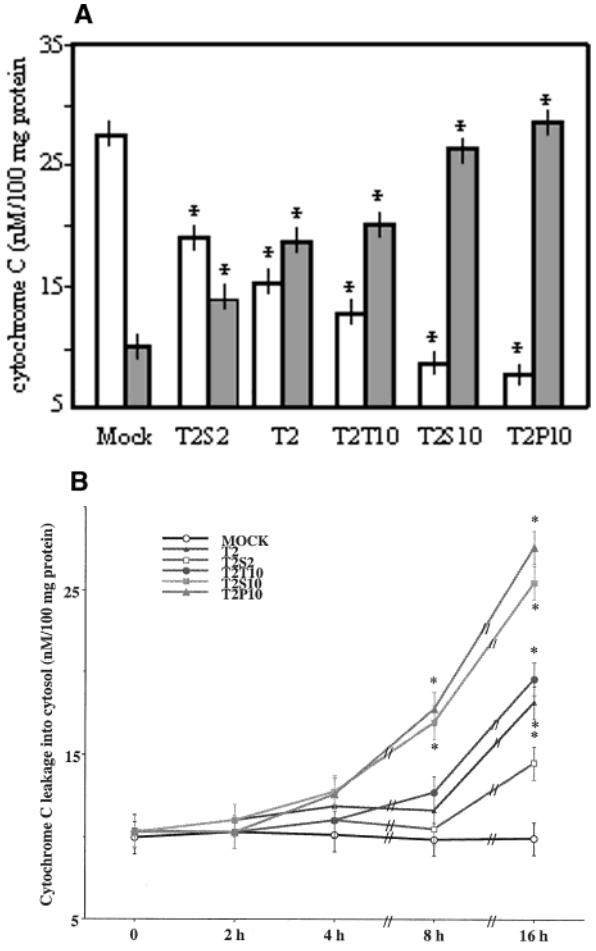

FIGURE 3: Histogramm shows cytochrome *c* concentrations in cytosolic fraction (dashed bars) and mitochondrial fraction (white bars) after 16 h treatment with 50 μM DA (A). *Significantly different to mock treatment for each fraction. ANOVA, 95% confidence, Fisher PLSD. Mean ×b1 SD based on $n = 6$. Graph shows temporal changes in cytosolic cytochrome *c* in the presence of 50 μM DA (B). *Significantly different to mock treatment. ANOVA, 95% confidence, Fisher PLSD. Mean ± SD based on $n = 6$.

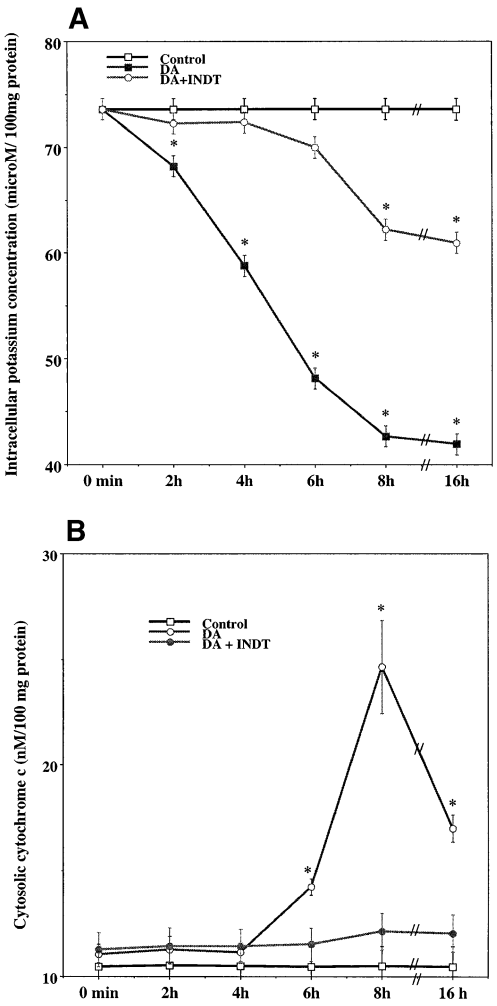

FIGURE 4: Graph shows temporal changes of intracellular potassium concentration in rat primary mesencephalic neurons treated with 10 μM DA (A) and temporal changes of cytosolic cytochrome *c* levels in rat primary mesencephalic neurons treated with 10 μM DA (B). *Significantly different to control. ANOVA, 95% confidence, Fisher PLSD. Mean ± SD based on $n = 5$.

[up to 6 h]. At 8 h of treatment, a breakdown in the ionic gradient was also observed in the indatraline-treated cells, although the loss in potassium was of much lower magnitude than that observed in the absence of the dopamine transporter blocker. Interestingly, the rate of decrease in intracellular potassium in neurons [$t_{1/2}$ of ~4.5 h] was somewhat slower than that seen in T2P10 cells [$t_{1/2}$ of ~3.5 h] but faster than that of T2S10 cells [$t_{1/2}$ of ~6.5 h]. Taken together, these data show that DA also causes loss of ionic gradient in primary mesencephalic neurons in a fashion similar to SH-SY5Y cells overexpressing the wt or the A30P α-synuclein but at a different time scale.

Measurement of cytosolic cytochrome *c* in primary mesencephalic neurons (Figure 4B) showed a significant increase in cytochrome *c* in the cytosol (50%) at 6 h in neurons treated with 10 μM DA, and this increase reached a peak (of ~150%) at 8 h, declining to about 75% after 16 h of treatment with DA. The decline in cytochrome *c* at 16 h is consistent with increased neuronal cell death and breakdown of cytochrome *c*. These data show that intracellular DA-induced changes in ionic gradient (2 h) precede leakage of cytochrome *c* from mitochondria (6 h) in α-synuclein expressing primary cultures of mesencephalic neurons further pointing to the physiological relevance of our findings in transfected SH-SY5Y cells and to a possible pathophysiological staging of neurotoxicity.

Metabolism of [3-^{13}C]Pyruvate in α-Synuclein Transfected SH-SY5Y Cells. Since alteration of mitochondrial function, evidenced by cytochrome *c* leakage, indicates a breakdown of the respiratory chain and depletion of metabolic energy, we confirmed this by evaluating the intermediate pool sizes [to measure rate of turnover] and flux [to measure incorporation of the label] of metabolites of select intermediates of the TCA cycle by NMR, using [3-^{13}C]pyruvate as a label, as described in Experimental Procedures.

Treatment of SH-SY5Y cells with 50 μM DA for 16 h resulted in a significant decrease in flux (Figure 5A) of ^{13}C label from [3-^{13}C]pyruvate into Succ C2/C3, Cit C2/C4, and Cit C3 in T2 cells as compared to mock cells, indicative of decreased mitochondrial TCA metabolism. However, in T2S2 cells, there was a significant reversal of this decrease in mitochondrial metabolism, indicative of a cytoprotective effect against DA toxicity, as compared to T2 cells. TCA metabolism was decreased in T2P10 (85%), followed by T2S10 (75%), and T2T10 (65%), further indicating a

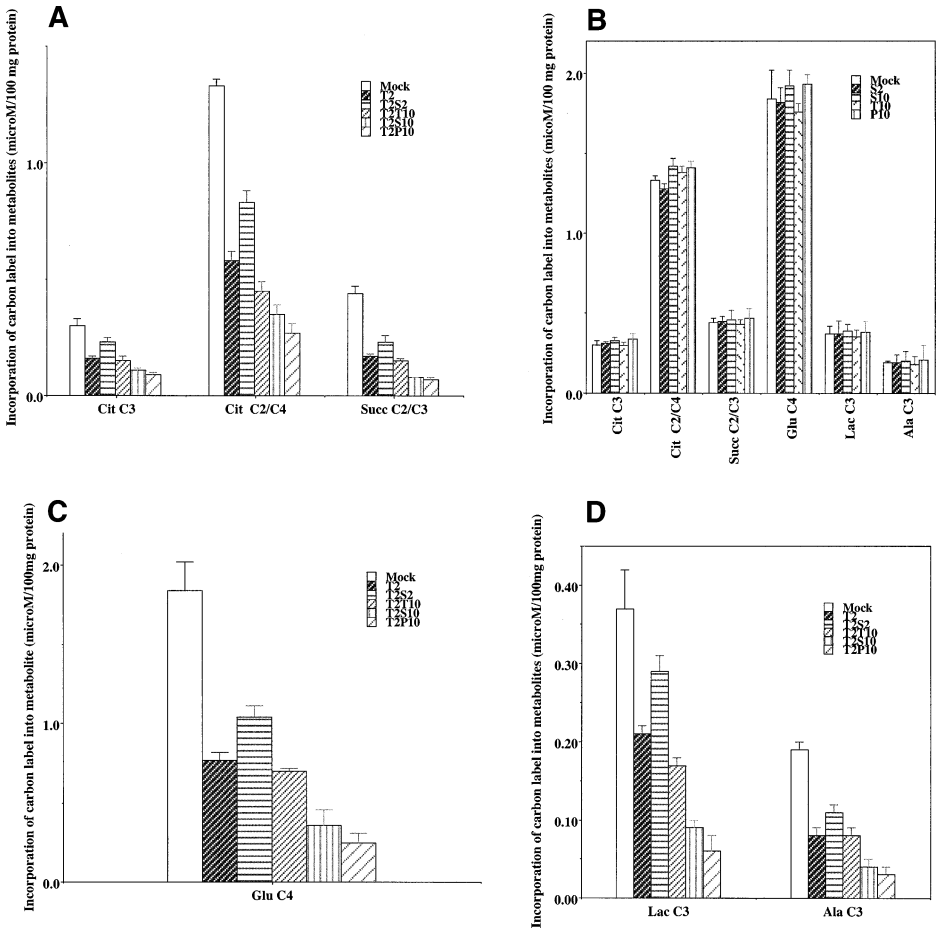

FIGURE 5: Histograms show incorporation of ^{13}C label from [3-^{13}C]pyruvate into citrate and succinate (A); citrate, succinate, glutamate, lactate, and alanine (B); glutamate (C); and lactate and alanine (D) in human neuroblastoma SH-SY5Y cells treated with 50 μM DA for 16 h. Cit: citrate; Succ: succinate; Glu: glutamate; Ala: alanine; and Lac: lactate. ANOVA, significance at 95%, Fisher PLSD. Mean ± SD based on $n = 4$.

differential effect for the various α-synuclein variants on mitochondrial metabolism. Moreover, treatment with 50 μM DA of SH-SY5Y cells transfected with the α-synuclein variants in the absence of DAT (Figure 5B) resulted in no noticeable changes in metabolic flux as compared to mock-treated cells, further indicating that α-synuclein effects on cytotoxicity are contingent upon the presence of intracellular DA. Taken together, the decrease in TCA metabolism indicates depletion of cellular metabolic energy and a possible impediment to global metabolism. Indeed, the observed decrease in flux of ^{13}C label from [3-^{13}C]pyruvate into Glu C4 (Figure 5C) had a pattern similar to TCA intermediates, succinate and citrate, confirming a decrease in global metabolism in the cell. Under the present experimental conditions, where the glutamate−glutamine cycle does not exist for recycling of cytosolic glutamate, labeled glutamate has a predominantly mitochondrial origin and is dependent on ATP to drive enzymatic reactions to convert the TCA intermediate α-ketoglutarate to glutamate.

Under conditions where mitochondrial metabolic energy is depleted, the cell may in part derive its energy from cytosolic sources including glycolysis and via the conversion of lactate to pyruvate, generating energy in the form of NADH. As glycolysis is omitted under the present experimental conditions due to glucose starvation, we examined whether the cell could use lactate and alanine as alternative energy substrates in the cytosol to compensate for the observed mitochondrial dysfunctions. Flux of ^{13}C label from [3-^{13}C]pyruvate into Lac C3 and Ala C3 (Figure 5D) was significantly decreased in T2 cells (45%) as compared to mock cells, while T2S2 reversed the effect of DA on metabolic flux of lactate and alanine to 75% of mock level but still resulted in a significant decrease (25%) as compared to mock cells. Flux of ^{13}C label from [3-^{13}C]pyruvate into cytosolic metabolites was most decreased in T2P10 (85%), followed by T2S10 (75%) and T2T10 (55%) as compared to mock cells. With the exception of flux of ^{13}C label from [3-^{13}C]pyruvate into Ala C3 and Glu C4 in T2 and T2T10 cells, all treatments were significantly different to each other. No noticeable changes were also observed in the flux of label into Lac C3 and Ala C3 in the absence of hDAT (Figure 5B). Furthermore, the changes in metabolic flux was echoed by fractional enrichment of individual isotopomers of metabolites (Table 1), further indicating differential effects of wt and mutant α-synuclein on cellular metabolism. Taken together, these data show a significant decrease in the reacting pool of all measured metabolites over 16 h of treatment with 50 μM DA, indicating an inhibitory effect on cellular metabolism and depletion of metabolic energy, thus increasing rate and extent of cell death.

While metabolic flux gives an indication of the size of the reacting pools of metabolites in the cell at any given time, measurement of the pool sizes or the nonreacting metabolic pools that maintain equilibrium in the cell give

Table 1: Percentage of Fractional Enrichment of Isotopomers in Human Neuroblastoma SH-SY5Y Cells Treated with 50 μM DA for 16 h[a]

	mock mean ± SD	T2S2 mean ± SD	T2 mean ± SD	T2T10 mean ± SD	T2S10 mean ± SD	T2P10 mean ± SD
Glu C4	7.8 ± 1.5	6.5 ± 0.4	5.6 ± 0.4	5 ± 0.5	2.5 ± 0.1	2.4 ± 0.1
Cit C3	0.5 ± 0.2	0.4 ± 0.01	0.3 ± 0.1	0.25 ± 0.02	0.16 ± 0.01	0.1 ± 0.01
Cit C2/C4	6.1 ± 1.3	5.3 ± 0.2	5 ± 0.5	4.5 ± 0.5	3.2 ± 0.3	3.1 ± 0.3
Succ C2/C3	1 ± 0.1	0.5 ± 0.1	0.4 ± 0.1	0.3 ± 0.09	0.19 ± 0.01	0.18 ± 0.02
Lac C3	3.9 ± 0.6	3.6 ± 0.5	3.1 ± 0.2	3.1 ± 0.1	2.9 ± 0.9	2.8 ± 0.7
Ala C3	2.1 ± 0.3	2 ± 0.4	1.7 ± 0.3	1.6 ± 0.2	1.1 ± 0.4	1.1 ± 0.4

[a] Cit: citrate; Succ: succinate; Glu: glutamate; Ala: alanine; and Lac: lactate. ANOVA, significance at 95%, Fisher PLSD. Mean ± SD based on $n = 4$.

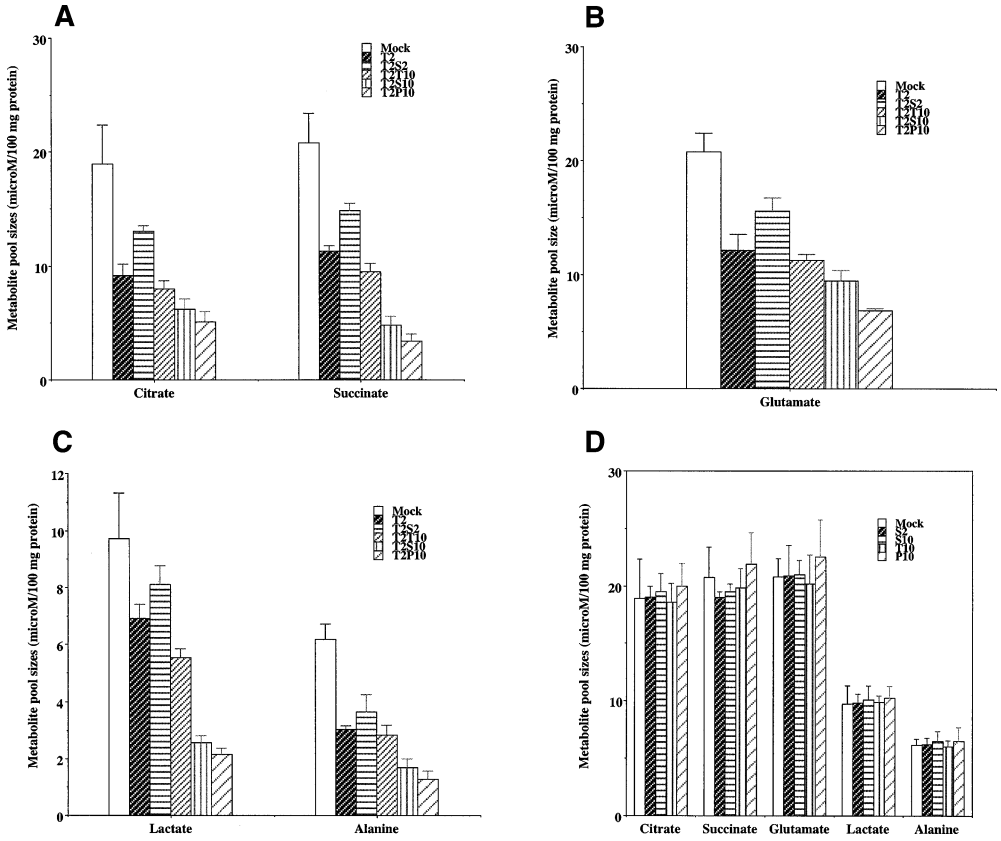

FIGURE 6: Histograms show total metabolite pool sizes of citrate and succinate (A); glutamate (B); lactate and alanine (C); and citrate, succinate, lactate, alanine, and glutamate (D) in human neuroblastoma SH-SY5Y cells treated with 50 μM DA for 16 h. ANOVA, significance at 95%, Fisher PLSD. Mean ± SD based on $n = 4$.

an indication of metabolic rate. Fluctuation in the equilibrium of cellular metabolites along with changes in metabolic flux indicate metabolic stress in the cell. Total metabolite pool sizes of citrate and succinate (Figure 6A) were significantly decreased in T2 cells (50%) as compared to mock cells, while the effect of DA was significantly reversed in T2S2 cells to 75% of the mock level, but this difference was still significantly different as compared to mock cells. The most dramatic decrease in the pool sizes of succinate and citrate was observed in T2P10 (75%) followed by T2S10 (70%) and T2T10 (55%) cells as compared to mock cells. These decreases in pool sizes indicate a significant decrease in TCA cycle turnover and decrease in energy production leading to depletion of metabolic energy. Furthermore, the pool size of glutamate (Figure 6B) followed almost an identical pattern, further indicating depletion of metabolic energy to drive global cellular metabolism. Pool sizes of cytosolic metabolite lactate (Figure 6C) was significantly decreased in T2 cells (30%) as compared to control, and T2S2 cells reversed the effects of DA to 80% of mock level, but this decrease was still significantly different to mock. Pool size of lactate was mostly decreased in T2P10 (85%), followed by T2S10 (80%) and T2T10 (50%) cells as compared to mock cells. However, the metabolic pool size of alanine was significantly decreased in T2 and T2T10 cells (50%) as compared to mock cells. The most dramatic decrease in alanine pool size was observed with T2P10 (70%) and T2S10 (65%) as compared to control. All treatments in these studies were significantly different to each other except the difference in alanine and glutamate between T2 and T2T10 and T2S10 and T2P10 in both alanine and lactate. Additionally, no significant differences were observed in cells transfected with the α-synuclein variants in the absence of hDAT (Figure 6D). Taken together, these studies suggest an inhibition of mitochondrial pools (50% T2, T2S2 25%, and 55% T2T10) of metabolites followed by inhibition of cytosolic pool (lactate 30% T2, T2S2 20%, and T2T10 50%) as indicated by the differential changes between cytosolic and mitochondrial compartments.

DISCUSSION

The present studies provide an insight into a possible pathological staging of progression of cytotoxicity and cell death induced by expression of α-synuclein in the presence of DA and indicate the differential effects of wt and mutant forms of α-synuclein on cellular properties and metabolism. Our data show the A30P mutant to be the most aggressive form of α-synuclein (*34*−*36*, *41*) to induce cell death, in terms of both time and magnitude, as compared to wt and the A53T mutant expressed at equal levels in the presence of intracellular DA. The data confirmed a possible cascade of events triggered initially by loss of ionic gradient, followed by leakage of cytochrome *c* from mitochondria into cytotosol, resulting ultimately in inhibition of metabolism and depletion of cellular energy, with subsequent cell death. The changes observed with intracellular potassium and mitochondrial damage are in perfect agreement with the decrease in cellular metabolism as shown by NMR. These data are consistent with previous observations showing the A30P mutant to be the slowest to oligomerize in vitro, perhaps leading to extended time of exposure to intermediate cytotoxic protofibrils, as compared to wt and A53T mutants (*44*−*46*). More importantly, oxidative injuries, which are linked to neurodegenerative diseases, include the nitration of tyrosine residues, and nitrated α-synuclein has been observed in LBs, or the formation of a DA-α-synuclein adduct (*20*, *33*). Moreover, it was recently shown that nitration of α-synuclein by DA inhibits fibrillation of human α-synuclein in vitro by formation of soluble oligomers (*47*). Taken together, these observations along with our data suggest that the selective death of dopaminergic neurons in PD may be caused by cellular stress from DA metabolism in the presence of α-synuclein. However, although the existence of α-synuclein oligomers in vivo is intriguing, it is still poorly understood how cytotoxic α-synuclein oligomers are formed or whether they form protofibrils in the same way as those described in in vitro systems (*44*−*46*). Thus, the absence of oligomerization of α-synuclein in our cellular system suggests that the possible toxicity of α-synuclein oligomers does not preclude a toxic insult from monomeric α-synuclein or possible formation of complex between α-synuclein with other proteins (*48*).

Cellular energy in the form of ATP is derived primarily from oxidative phosphorylation and the TCA cycle providing the driving force for life in the cell. Leakage of cytochrome *c* into cytosol indicates impairment of the mitochondrial electron-transfer chain and breakdown of oxidative phosphorylation, thus the inhibition of TCA cycle metabolism. Additionally, Na^+/K^+-ATPase is a target of oxygen-centered free radicals (*49*−*56*), such as those produced by DA metabolism and α-synuclein (*51*, *54*, *56*, *57*). Therefore, inhibition of Na^+/K^+-ATPase pump by ROS under the present experimental conditions may have a significant contribution to the overall changes in ionic gradient. Moreover, changes in ionic gradient with high expression levels of wt and A30P forms of α-synuclein seem to reach a level at which the Na^+/K^+-ATPase pump activity was affected in an identical manner to cells treated with ouabain. Furthermore, Na^+/K^+-ATPase pump, which largely maintains cellular ionic gradients, is energy dependent, and the decrease in TCA cycle metabolism is evidenced by the decrease in the metabolism of citrate and succinate, two intermediates of the mitochondrial TCA cycle, which is indicative that the cell major energy supplies are depleted. That suggests that ROS production and ATP depletion may have cumulative effects on down-regulating the activity of the Na^+/K^+-ATPase pump leading to further loss of cellular ionic gradient. Additionally, the loss of ionic gradient seems to be DA-dependent and α-synuclein-induced under the present experimental conditions, further suggesting that the cell death triggered in SH-SY5Y cells may result from damage to membrane lipids, causing a loss of cellular ionic gradient (*8*−*14*, *57*). Furthermore, although a low expression level of wt α-synuclein has a protective effect against DA toxicity (*13*, *14*, *38*), low expression levels of α-synuclein can cause oxidative damage, even in the absence of α-synuclein mutation or overexpression, over a protracted time course (*37*). Similarly, the data also show that intracellular DA-induced changes in ionic gradient (2 h) precede leakage of cytochrome *c* from mitochondria into cytosol (6 h) in α-synuclein expressing primary cultures of mesencephalic neurons, further pointing to the physiological relevance of our data and to a possible pathophysiological staging of neurotoxicity.

Under conditions of shortage of metabolic energy, lactate would be a particularly favorable substrate for energy since it is readily converted to pyruvate by lactate dehydrogenase (LDH), providing immediate energy in the form of NADH, and also providing a source of acetyl CoA for maintaining TCA cycle activity (*58*, *59*). It should be noted, however, that the ability of SH-SY5Y neuroblastoma cells to utilize lactate depends on the activity of the malate−aspratate shuttle to maintain cytosolic NAD^+ required for LDH activity (*59*, *60*). Therefore, the decrease in metabolism of lactate may suggest that lactate, instead of being metabolized through the TCA cycle, perhaps serves as a substrate for replenishing energy requirements (*61*−*67*). Additionally, several metabolites can serve as energy substrates including lactate, alanine, and glutamine (*68*). Thus, the decrease in alanine metabolism is also indicative of depletion of metabolic energy. Nonetheless, the observed decrease in glutamate metabolism and MTT reduction by cellular dehydrogenases, which need NADH to function, suggest an overall decrease in cellular metabolism. Taken together, the decrease in metabolism observed in the present studies is consistent with previous evidence pointing to reduced cerebral metabolism in the clinically presymptomatic PD patients, suggesting that decreased energy metabolism precedes clinical symptoms, which appear after 70−80% death of dopaminergic nigral neurons (*69*). Furthermore, hypometabolism was also found in the striata of advanced cases of PD patients without dementia (*70*, *71*) and in the cortex of PD patients who were affected at the cognitive level (*71*). In contrast to clinically advanced cases, early and mildly affected PD patients showed striatal hypermetabolism (*72*, *73*). Additionally, it is worth it to mention several reports indicating systematic reductions in the activity of the electron-transfer chain in PD patients (*72*−*74*). Indeed, MTT assays in the present studies show increased cell death in parallel to increased mitochondrial impairment and decreased metabolism, suggesting that changes in cellular metabolism may precede cell death.

The present studies raise an important question regarding the mechanisms by which hDAT activity may be regulated,

particularly since the Na^+/Cl^--dependent hDAT stoichiometry dictates that DA uptake can be maintained under conditions when transmembrane ion gradients are all maintained by membrane Na^+/K^+-ATPases (*75*), strongly suggesting that changes in both ionic gradient and intracellular ATP concentration can influence hDAT function, thus leading to decreased uptake of DA. Furthermore, cultured astrocytes and cell lines maintain a high energy level through operation of oxidative phosphorylation and glycolysis, which contribute 25−32% of total ATP production, via maintenance of ionic equilibrium by the Na^+/K^+-ATPase pump; however, a decrease in pump activity via a fall in ATP concentration collapses ion gradients (*76*). Glycolysis (and glutaminolysis) is omitted under the present experimental conditions, leaving oxidative phosphorylation and TCA cycle as the main sources of metabolic energy. Therefore, the present studies prompted this hypothesis pertaining to regulation of hDAT activity under similar conditions, and it is currently under intensive investigation in our laboratory.

In conclusion, the present studies have provided an unprecedented insight into the metabolic and cellular mechanisms underlying α-synuclein cytotoxicity in the presence of intracellular DA, suggesting that high expression levels of the wt and mutant forms α-synuclein cause an increase in ROS production and changes in ionic gradients, at different times, resulting in mitochondrial impairment, reduced metabolism, depletion of metabolic energy, and subsequent cell death.

ACKNOWLEDGMENT

The authors gratefully acknowledge the support of the National Magnetic Resonance Facilities at Madison (NMRFAM), University of Wisconsin−Madison, for allowing the NMR studies to be conducted there.

REFERENCES

1. Pollanen, M. S., Dickson, D. W., and Bergeron, C. (1993) Pathology and biology of the Lewy body, *J. Neuropathol. Exp. Neurol. 52*, 183−191.
2. Jakes, R., Spillantini, M. G., and Goedert, M. (1994) Identification of two distinct synucleins from human brain, *FEBS Lett. 354* (1), 27−32.
3. Forno, L. S. (1996) Neuropathology of Parkinson's disease, *J. Neuropathol. Exp. Neurol. 55*, 259−272.
4. Spillantini, M. G., Crowther, R. A., Jakes, R., Hasegawa, M., and Goedert, M. (1998) α-Synuclein in filamentous inclusions of Lewy bodies from Parkinson's disease and dementia with Lewy bodies, *Proc. Natl. Acad. Sci. U.S.A. 95* (11), 6469−6473.
5. Dunnett, S. B., and Bjorklund, A. (1999) Prospects for new restorative and neuroprotective treatments in Parkinson's disease, *Nature 399*, A32−A39.
6. Masliah, E., Rockenstein, E., Veinbergs, I., Mallory, M., Hashimoto, M., Takeda, A., Sagara, Y., Sisk, A., and Mucke, L. (2000) Dopaminergic loss and inclusion body formation in α-synuclein mice: implications for neurodegenerative disorders, *Science 287*, 1265−1269.
7. Feany, M. B., and Bender, W. W. (2000) A *Drosophila* model of Parkinson's disease, *Nature 404* (6776), 394−398.
8. Dexter, D. T., Carter, C. J., Wells, F. R., Javoy-Agid, F., Agid, Y., Lees, A., Jenner, P., and Marsden, C. D. (1989) Basal lipid peroxidation in substantia nigra is increased in Parkinson's disease, *J. Neurochem. 52*, 302−306.
9. Sian, J., Dexter, D. T., Lees, A. J., Daniel, S., Agid, Y., Javoy-Agid, F., Jenner, P., and Marsden, C. D. (1994) Alterations in glutathione levels in Parkinson's disease and other neurodegenerative disorders affecting basal ganglia, *Ann. Neurol. 36*, 348−355.
10. Alam, Z. I., Daniel, S. E., Lees, A. J., Marsden, C. D., Jenner, P., and Halliwell, B. (1997) A generalized increase in protein carbonyls in the brain in Parkinson's but not incidental Lewy body disease, *J. Neurochem. 69*, 1326−1329.
11. Pearce, R. K., Owen, A., Daniel, S., Jenner, P., and Marsden, C. D. (1997) Alterations in the distribution of glutathione in the substantia nigra in Parkinson's disease, *J. Neural. Trans. 104*, 661−677.
12. Floor, E., and Wetzel, M. G. (1998) Increased protein oxidation in human substantia nigra pars compacta in comparison with basal ganglia and prefrontal cortex measured with an improved dinitrophenylhydrazine assay, *J. Neurochem. 70*, 268−275.
13. Hasegawa, E., Takeshige, K., Oishi, T., Murai, Y., and Minakami, S. (1990) 1-Methyl-4-phenylpyridinium (MPP^+) induces NADH-dependent superoxide formation and enhances NADH-dependent lipid peroxidation in bovine heart submitochondrial particles, *Biochem. Biophys. Res. Commun. 170*, 1049−1055.
14. Lotharius, J., and O'Malley, K. L. (2000) The Parkinsonism-inducing drug 1-methyl-4-phenylpyridinium triggers intracellular dopamine oxidation. A novel mechanism of toxicity, *J. Biol. Chem. 275*, 38581−38588.
15. Crowther, R. A., Jakes, R., Spillantini, G. M., and Goerdert. M. (1998) Synthetic filaments assembled from C-terminally truncated α-synuclein, *FEBS Lett. 436* (*3*), 309−312.
16. El-Agnaf, O. M. A., Jakes, R., Curran, M. D., and Wallace, A. (1998) Effects of the mutations Ala30 to Pro and Ala53 to Thr on the physical and morphological properties of α-synuclein protein implicated in Parkinson's disease, *FEBS Lett. 440* (1−2), 67−70.
17. Gosavi, N., Lee, H. J., Lee, J. S., Patel, S., and Lee, S. J. (2002) Golgi fragmentation occurs in the cells with prefibrillar α-synuclein aggregates and precedes the formation of fibrillar inclusions, *J. Biol. Chem. 277* (50), 48984−48992.
18. Lashuel, H. A., Hartley, D., Petre, B. M., Walz, T., and Lansbury, P. T., Jr. (2002) Neurodegenerative disease: amyloid pores from pathogenic mutations, *Nature 418*, 291−292.
19. Lashuel, H. A., Petre, B. M., Wall, J., Simon, M., Nowak, R. J., Walz, T., and Lansbury, P. T., Jr. (2002) α-synuclein, especially the Parkinson's disease-associated mutants, form pore-like annular and tubular protofibrils, *J. Mol. Biol. 322*, 1089−1102.
20. Souza, J. M., Giasson, B. I., Chen, Q., Lee, V. M., and Ischiropoulos, H. (2000) Dityrosine cross-linking promotes formation of stable α-synuclein polymers. Implication of nitrative and oxidative stress in the pathogenesis of neurodegenerative synucleinopathies, *J. Biol. Chem. 275*, 18344−18349.
21. Turnbull, S., Tabner, B. J., El-Agnaf, O. M. A., Moore, S., Davies, Y., and Allsop D. (2001) α-Synuclein implicated in Parkinson's disease catalyzes the formation of hydrogen peroxide in vitro, *Free Radical Biol. Med. 30*(10), 1163−1170.
22. Kruger, R., Kuhn, W., Leenders, K. L., Sprengelmeyer, R., Muller, T., Woitalla, D., Portman, A. T., Maguire, R. P., Veenma, L., Schroder, U., Schols, L., Epplen, J. T., Riess, O., and Przuntek, H. (2001) Familial parkinsonism with synuclein pathology: clinical and PET studies of A30P mutation carriers, *Neurology 56* (10), 1355−1362.
23. Trojanowski, J. Q., Goedert, M., Iwatsubo, T., and Lee, V. M. (1998) Fatal attractions: abnormal protein aggregation and neuron death in Parkinson's disease and Lewy body dementia, *Cell Death. Differ. 5* (10), 832−837.
24. Braak, H., Del Tredici, K. D., Rub, U., de Vos, R. A. I., Jansen Steur, E. N., and Braak, E. (2003) Staging of brain pathology related to sporadic Parkinson's disease, *Neurobiol. Aging 24* (2), 197−211.
25. Dekker, M. C., Bonifati, V., and Van Duijn, C. M. (2003) Parkinson's disease: piecing together a genetic jigsaw, *Brain 126*, 1722−1733.
26. Polymeropoulos, M. H., Lavedon, C., Leroy, E., Ide, S. E., Dehejia, A., Dutra, A., Pike, B., Root, H., Rubenstein, J., Boyer, R., Stenroos, E. S., Chandrasekharappa, S., Athanassiadou, A., Papapetropoulos, T., Johnson, W. G., Lazzarini, A. M., Duvoisin, R. C., Di Iorio, G., Golbe, L. I., and Nussbaum, R. L. (1997) Mutation in the α-synuclein gene identified in families with Parkinson's disease, *Science 276*, 2045−2047.
27. Kruger, R., Kuhn, W., Muller, T., Woitalla, D., Graeber, M., Kosel, S., Przuntek, H., Epplen, J. T., Schols, L., and Reiss, O. (1998) Ala30Pro mutation in the gene encoding α-synuclein in Parkinson's disease, *Nat. Genet. 18*, 106−108.
28. Narhi, L., Wood, S. J., Steavenson, S., Jiang, Y., Wu, G. M., Anafi, D., Kaufman, S. A., Martin, F., Sitney, K., Denis, P., Louis, J.-

C., Wypych, J., Biere, A. L., and Citron, M. (1999) Both familial Parkinson's disease mutations accelerate α-synuclein aggregation, *J. Biol. Chem. 274* (1), 9843−9846.
29. Giasson, B. I., Uryu, K., Trojanowski, J. Q., and Lee, V. M. Y. (1999) Mutant and wild-type human α-synucleins assemble into elongated filaments with distinct morphologies in vitro, *J. Biol. Chem. 274* (12), 7619−7622.
30. Li, J., Uversky, V. N., and Fink, A. L. (2001) Effect of familial Parkinson's disease point mutations A30P and A53T on the structural properties, aggregation, and fibrillation of human α-synuclein, *Biochemistry 40* (38), 11604−11613.
31. Conway, K. A., Lee, S. J., Rochet, J. C., Ding, T. T., Williamson, R. E., and Lansbury, P. T., Jr. (2000) Acceleration of oligomerization, not fibrillization, is a shared property of both α-synuclein mutations linked to early-onset Parkinson's disease: implications for pathogenesis and therapy, *Proc. Natl. Acad. Sci. U.S.A. 97* (2), 571−576.
32. Uversky, V. N., Li, J., and Fink, A. L. (2001) Evidence for a partially folded intermediate in α-synuclein fibril formation, *J. Biol. Chem. 276* (14), 10737−10744.
33. Conway, K. A., Rochet, J. C., Bieganski, R. M., and Lansbury. P. T., Jr. (2001) Kinetic stabilization of the α-synuclein protofibril by a dopamine-α-synuclein adduct, *Science 294* (5545), 1346−1349.
34. Conway, K. A., Harper, J. D., and Lansbury, P. T., Jr. (1998) Accelerated in vitro fibril formation by a mutant α-synuclein linked to early-onset Parkinson disease, *Nat. Med. 4* (11), 1318−1320.
35. Rochet, J. C., Conway, K. A., and Lansbury, P. T., Jr. (2000) Inhibition of fibrillization and accumulation of prefibrillar oligomers in mixtures of human and mouse α-synuclein, *Biochemistry 39* (35), 10619−10626.
36. Haass, C., and Kahle, P. J. (2000) Parkinson's pathology in a fly, *Nature 404*, 341−343.
37. Hsu, L. J., Sagara, Y., Arroyo, A., Rockenstein, E., Sisk, A., Mallory, M., Wong, J., Takenouchi, T., Hashimoto, M., and Masliah, E. (2000) α-synuclein promotes mitochondrial deficit and oxidative stress, *Am. J. Pathol. 157* (2), 401−410.
38. Sherer, T. B., Betarbet, R., Stout, A. K., Lund, S., Baptista, M., Panov, A. V., Cookson, M. R., and Greenamyre, J. T. (2002) An in vivo model of Parkinson's disease: linking mitochondrial impairment to altered α-synuclein metabolism and oxidative damage, *J. Neurosci. 22* (15), 7006−7015.
39. Seo, J.-H., Rah, J.-C., Choi, S. H, Shin, J. K., Min, K., Kim, H. S., Park, C. H., Kim, S., Kim, E. M., Lee, S. H., Lee, S., Suh, S. W., and Suh, Y. H. (2002) α-synuclein regulates neuronal survival via Bcl-2 family expression and PI3/Akt kinase pathway, *FASEB J. 16*, 1826−1828.
40. Wersinger, C., and Sidhu, A. (2003) Attenuation of dopamine transporter activity by α-synuclein, *Neurosci. Lett. 340* (3), 189−192.
41. Wersinger, C., Prou, D., Vernier P., and Sidhu, A. (2003) Modulation of dopamine transporter function by α-synuclein is altered by impairment of cell adhesion and by induction of oxidative stress, *FASEB J. 17* (14), 2151−2153.
42. Wersinger, C., Prou, D., Vernier P., Niznik, H. B., and Sidhu, A. (2003) Mutations in the lipid-binding domain of α-synuclein confer overlapping, yet distinct, functional properties in the regulation of dopamine transporter activity, *Mol. Cell. Neurosci. 24* (1), 91−105.
43. Sonnewald, U., Westergaard, N., Hassel, B., Muller, T. B., Unsgard, G., Fonnum, F., Hertz, L., Schousboe, A., and Petersen, S. B. (1993) NMR spectroscopic studies of 13C acetate and 13C glucose metabolism in neocortical astrocytes: evidence for mitochondrial heterogeneity, *Dev. Neurosci. 15*, 351−358.
44. Goldberg, M. S., and Lansbury. P. T., Jr. (2000) Is there a cause-and-effect relationship between α-synuclein fibrillization and Parkinson's disease? *Nat. Cell Biol. 2*, E115−E119.
45. Kayed, R., Head, E., Thompson, J. L., McIntire, T. M., Milton, S. C., Cotman, C. W., and Glabe, C. G. (2003) Common structure of soluble amyloid oligomers implies common mechanism of pathogenesis, *Science 300*, 486−489.
46. Bucciantini, M., Giannoni, E., Chiti, F., Baroni, F., Formigli, L., Zurdo, J., Taddei, N., Ramponi, G., Dobson, C. M., and Stefani, M. (2002) Inherent toxicity off aggregates implies a common mechanism for protein misfolding diseases, *Nature 416*, 507−511.
47. Yamin, G., Uversky, V. N., and Fink, A. L. (2003) Nitration inhibits fibrillation of human α-synuclein in vitro by formation of soluble oligomers, *FEBS Lett. 542*, 147−152.
48. Welch, K., and Yuan, J. (2003) α-synuclein oligomerization: a role for lipids? *Trends Neurosci. 26* (10), 517−519.
49. Rohn, T. T., Hinds, T. R., and Vincenzi, F. F. (1996) Inhibition of Ca2+-pump ATPase and the Na+/K+-pump ATPase by iron-generated free radicals. Protection by 6,7-dimethyl-2,4-DI-1-pyrrolidinyl-7H-pyrrolo[2,3-d] pyrimidine sulfate (U-89843D), a potent, novel, antioxidant/free radical scavenger, *Biochem. Pharmacol. 51* (4), 471−476.
50. Gilbert, M., and Knox, S. (1997) Influence of Bcl-2 overexpression on Na+/ K(+)-ATPase pump activity: correlation with radiation-induced programmed cell death, *J. Cell. Physiol. 171* (3), 299−304.
51. Kourie, J. I. (1998) Interaction of reactive oxygen species with ion transport mechanisms, *Am. J. Physiol. 275* (Pt 1), C1−C24.
52. Bulygina, E. R., Lyapina, L. Y., and Boldyrev, A. A. (2002) Activation of glutamate receptors inhibits Na/K-ATPase of cerebellum granule cells, *Biochemistry (Moscow) 67* (9), 1001−1005.
53. Tanaka, K., Weihrauch, D., Ludwig, L. M., Kersten, J. R., Pagel, P. S., and Warltier, D. C. (2003) Mitochondrial adenosine triphosphate-regulated potassium channel opening acts as a trigger for isoflurane-induced preconditioning by generating reactive oxygen species, *Anesthesiology 98* (4), 935−943.
54. Xie, Z., and Askari, A. (2002) Na(+)/K(+)-ATPase as a signal transducer, *Eur. J. Biochem. 269* (10), 2434−2439.
55. Dada, L. A., Chandel, N. S., Ridge, K. M., Pedemonte, C., Bertorello, A. M., and Sznajder, J. I. (2003) Hypoxia-induced endocytosis of Na/K-ATPase in alveolar epithelial cells is mediated by mitochondrial reactive oxygen species and PKC-zeta, *J. Clin. Invest. 117* (7), 1057−1064.
56. Xie, Z. (2003) Molecular mechanisms of Na/K-ATPase-mediated signal transduction, *Ann. N. Y. Acad. Sci. 986*, 497−503.
57. Xu, J., Kao, S. Y., Lee, F. J., Song, W., Jin, L. W., and Yankner, B. A. (2002) Dopamine-dependent neurotoxicity of α-synuclein: a mechanism for selective neurodegeneration in Parkinson's disease, *Nat. Med. 8*, 600−606.
58. Bittar, P. G., Charnay, Y., Pellerin, L., Bouras, C., and Magistretti, P. J. (1996) Selective distribution of lactate dehydrogenase isoenzymes in neurons and astrocytes of human brain, *J. Cereb. Blood. Flow. Metab. 16* (6), 1079−1089.
59. Anderson, C. M., and Swanson, R. A. (2000) Astrocyte glutamate transport: review of properties, regulation, and physiological functions, *Glia 32* (1), 1−14.
60. McKenna, M. C., Tildon, J. T., Stevenson, J. H., Jr., Boatright, R., and Huang, S. (1993) Regulation of energy metabolism in synaptic terminals and cultured rat brain astrocytes: differences revealed using aminooxyacetate, *Dev. Neurosci. 15*, 320−329.
61. Medina, J. M. (1985) The role of lactate as an energy substrate for the brain during the early neonatal period, *Biol. Neonate 48* (4), 237−244.
62. McKenna, M. C., Tildon, J. T., Stevenson, J. H., and Hopkins, I. B. (1994) Energy metabolism in cortical synaptic terminals from weanling and mature rat brain: evidence for multiple compartments of tricarboxylic acid cycle activity, *Dev. Neurosci. 16*, 291−300.
63. Schurr, A., West, C. A., and Rigor, B. M. (1988) Lactate-supported synaptic function in the rat hippocampal slice preparation, *Science 240*, 1326−1328.
64. Waagepetersen, H. S., Bakken, I. J., Larsson, O. M., Sonnewald, U., and Schousboe, A. (1998) Metabolism of lactate in cultured GABAergic neurons studied by 13C nuclear magnetic resonance spectroscopy, *J. Cereb. Blood. Flow. Metab. 18* (1), 109−117.
65. Waagepetersen, H. S., Bakken, I. J., Larsson, O. M., Sonnewald, U., and Schousboe, A. (1998) Comparison of lactate and glucose metabolism in cultured neocortical neurons and astrocytes using ^{13}C NMR spectroscopy, *Dev. Neurosci. 20*, 310−320.
66. Schurr, A., West, C. A., and Rigor, B. M. (1989) Electrophysiology of energy metabolism and neuronal function in the hippocampal slice preparation, *J. Neurosci. Methods 28* (1−2), 7−13.
67. Bouzier, A. K., Thiaudiere, E., Biran, M., Roulard, R., Canioni, P., and Merle, M. (2000) The metabolism of [3-(13)C]lactate in the rat brain is specific of a pyruvate carboxylase-deprived compartment, *J. Neurochem. 75* (2), 480−486.
68. Poitry-Yamate, C. L., Vutskits, L., and Rauen, T. (2002) Neuronal-induced and glutamate-dependent activation of glial glutamate transporter function, *J. Neurochem. 82* (4), 987−997.

69. Berding, G., Odin, P., Brooks, D. J., Nikkhah, G., Matthies, C., Peschel, T., Shing, M., Kolbe, H., van Den Hoff, J., Fricke, H., Dengler, R., Samii, M., and Knapp, W. H. (2001) Resting regional cerebral glucose metabolism in advanced Parkinson's disease studied in the off and on conditions with [(18)F]FDG-PET, *Neurology 2* (3), 1355−1362.
70. Peppard, R. F., Martin, W. R., Carr, G. D., Grochowski, E., Schulzer, M., Guttman, M., McGeer, P. L., Phillips, A. G., Tsui, J. K., and Calne, D. B. (1992) Cerebral glucose metabolism in Parkinson's disease with and without dementia, *Arch. Neurol. 49* (12), 1262−1268.
71. Eidelberg, D., Moeller, J. R., Ishikawa, T., Dhawan, V., Spetsieris, P., Chaly, T., Belakhlef, A., Mandel, F., Przedborski, S., and Fahn, S. (1995) Early differential diagnosis of parkinson's disease with 18F-fluorodeoxyglucose and positron emission tomography, *Neurology 45* (11), 1995−2004.
72. Parker, W. D., Jr., Boyson, S. J., and Parks, J. K. (1989) Abnormalities of the electron transport chain in idiopathic Parkinson's disease, *Ann. Neurol. 26* (6), 719−723.
73. Mizuno, Y., Ohta, S., Tanaka, M., Takamyia, S., Suzuki, K., Sato, T., Oya, H., Ozawa, T., and Kagawa, Y. (1989) Deficiencies in complex I subunits of the respiratory chain in Parkinson's disease, *Biochem. Biophys. Res. Commun. 163* (3), 1450−1455.
74. Schapira, A. H., Cooper, J. M., Dexter, D., Jenner, P., Clark, J. B., and Marsden, C. D. (1989) Mitochondrial complex I deficiency in Parkinson's disease, *Lancet 1* (8649), 1269.
75. Nelson, N. (1998) The family of Na^+/Cl^- neurotransmitter transporters, *J. Neurochem. 71*, 1785−1803.
76. Silver, I. A., and Erecinska, M. (1997) Energetic demands of the Na^+/K^+ ATPase in mammalian astrocytes, *Glia 21* (1), 35−45.

BI036114F